Biosci. Rep. (2012) / **32** / 587–595 (Printed in Great Britain) / doi 10.1042/BSR20120085

online data

Original Paper

Bafilomycin A1 activates HIF-dependent signalling in human colon cancer cells via mitochondrial uncoupling

Alexander V. ZHDANOV[1], Ruslan I. DMITRIEV and Dmitri B. PAPKOVSKY

Biochemistry Department, University College Cork, Cork, Ireland

Synopsis

Mitochondrial uncoupling is implicated in many patho(physiological) states. Using confocal live cell imaging and an optical O_2 sensing technique, we show that moderate uncoupling of the mitochondria with plecomacrolide Baf (bafilomycin A1) causes partial depolarization of the mitochondria and deep sustained deoxygenation of human colon cancer HCT116 cells subjected to 6% atmospheric O_2. A decrease in iO_2 (intracellular O_2) to 0–10 μM, induced by Baf, is sufficient for stabilization of HIFs (hypoxia inducible factors) HIF-1α and HIF-2α, coupled with an increased expression of target genes including GLUT1 (glucose transporter 1), HIF PHD2 (prolyl hydroxylase domain 2) and CAIX (carbonic anhydrase IX). Under the same hypoxic conditions, treatment with Baf causes neither decrease in iO_2 nor HIF-α stabilization in the low-respiring HCT116 cells deficient in COX (cytochrome *c*-oxidase). Both cell types display equal capacities for HIF-α stabilization by hypoxia mimetics DMOG (dimethyloxalylglycine) and $CoCl_2$, thus suggesting that the effect of Baf under hypoxia is driven mainly by mitochondrial respiration. Altogether, by activating HIF signalling under moderate hypoxia, mitochondrial uncoupling can play an important regulatory role in colon cancer metabolism and modulate adaptation of cancer cells to natural hypoxic environments.

Key words: bafilomycin A1, bioenergetics, hypoxia inducible factor, intracellular oxygen, mitochondrial function, respiration.

Cite this article as: Zhdanov, A. V., Dmitriev, R. I. and Papkovsky, D. B. (2012) Bafilomycin A1 activates HIF-dependent signalling in human colon cancer cells via mitochondrial uncoupling. Biosci. Rep. **32**, 587–595

INTRODUCTION

Plecomacrolide Baf (bafilomycin A1) [1], known as a potent inhibitor of the V-ATPase (vacuolar H^+-ATPase) [2–4], regulates a number of metabolic processes associated with translocation of protons into the acidic compartments. Treatment with Baf causes lysosome dysfunction, decrease in pH and elevation of cytosolic Ca^{2+}, and neurotransmission failure in neural cells [5–10], which, in turn, induces permeability transition pore opening [11] and cell death. Impaired fusion of autophagosomes with dysfunctional lysosomes inhibits autophagy [12] and triggers apoptosis [13] and therefore is considered to be one of the main mechanisms of the anticancer effect of Baf. In agreement with pro-apoptotic properties, Baf and another V-ATPase inhibitor CMA (concanamycin A) were also shown to induce mitochondrial depolarization and apoptosis in leukaemic monocytes by activating the production of nitric oxide [14].

Anti-cancer effects of Baf connect V-ATPase and HIF-1 (hypoxia inducible factor 1) [15–17]. Baf was shown to promote direct interaction of V0 subunit *c* (ATP6V0C) with HIF-1α and its stabilization, which, in turn, induced $p21^{WAF1/Cip1}$-mediated growth arrest in a number of cancer cell lines [15–17]. ATP6V0C protects HIF-1α from interaction with VHL (von Hippel–Lindau) E3 ubiquitin ligase and subsequent proteasomal degradation. In normoxia HIF-α subunits are maintained at low levels. Upon hydroxylation by O_2-dependent prolyl and asparaginyl hydroxylases [PHD (prolyl hydroxylase domain) 1–4 and

Abbreviations used: AA, antimycin A; Baf, bafilomycin A1; CAIX, carbonic anhydrase IX; CMA, concanamycin A; COX, cytochrome *c* oxidase; $\Delta\Psi$m, membrane potential; DAPI, 4′,6-diamidino-2-phenylindole; DIC, differential interference contrast; DMOG, dimethyloxalylglycine; FIH, factor inhibiting HIF; GLUT1, glucose transporter 1; HIF, hypoxia inducible factor; HRE, hypoxia response element; HRP, horseradish peroxidase; iO_2, intracellular O_2; MTG, Mito Tracker® Green; OCR, O_2 consumption rate; PDL, poly-D-lysine; PHD, prolyl hydroxylase domain; RT, reverse transcription; SCO2, synthesis of COX 2; TR-F, time-resolved fluorescence; TMRM, tetramethyl rhodamine methyl ester; UCP, uncoupling protein; V-ATPase, vacuolar H^+-ATPase; VDAC1, voltage-dependent anion channel 1; VHL, von Hippel–Lindau; WT, wild-type.

[1] To whom correspondence should be addressed (email a.zhdanov@ucc.ie).

FIH (factor inhibiting HIF)], HIF-α subunits undergo degradation through VHL protein or lose their DNA binding capacity [18]. The rate of HIF-α degradation decreases at low O_2 (hypoxia) and α-ketoglutarate availability, or upon pharmacological inhibition of PHDs [19].

Identifying new molecules targeting HIFs is of high practical interest, because HIFs regulate cancer cell metabolism and tumour progression [20]. The majority of therapeutic compounds targeting cancer via HIF signalling have an inhibitory effect on HIF stabilization/transactivation (see [21]). However, the results on Baf-dependent cancer suppression mediated by HIF-1 contradict the role of HIF-1α as a transcriptional regulator of cancer cell survival and progression of many tumours [20], including colon cancer [22–24]. In solid tumours, deep deoxygenation [25] contributes to HIF-1α stabilization, the latter promotes cancer development through VEGF (vascular endothelial growth factor)-dependent vascularization and pro-glycolytic rearrangement of cell metabolism [20]. Surprisingly, expression of common HIF-1 targeted genes was not affected by Baf [17].

Despite the remarkable effect of Baf on HIF-1α, stabilization of HIF-2α and its role in Baf-dependent cancer suppression has not been analysed. Yet, the unique transcriptional signatures of HIF-1 and HIF-2 make them very specific regulators of tumour progression. Thus, HIF-2 is associated with malignant tumours and poor survival prognosis [26–29], while accumulation of HIF-1α in a number of HIF-2-associated tumours was linked to decreased patient mortality [30,31].

The recently found uncoupling effect of Baf on isolated mitochondria [32] and neuronal cells [33] may also contribute to stabilization of HIF-α subunits by activating respiration and decreasing iO_2 (intracellular O_2) levels. Indeed, it is known that increased mitochondrial activity regulates HIF-α stabilization in an iO_2-dependent manner [34–37]. Knowing that relative oxygenation of respiring cells decreases at reduced O_2 availability [38], we hypothesized that at physiological O_2 levels (2–12% O_2), treatment with Baf can shift cell deoxygenation to levels sufficient for HIF-1α and HIF-2α stabilization. To check this, we compared the effect of Baf on HIF signalling in two human colon cancer cell lines, exposed to 6% O_2 for 5 h. As models we used actively respiring WT (wild-type) HCT116 cells and low respiring HCT116 cells deficient in SCO2 protein (synthesis of COX 2, which is involved in the COX (cytochrome *c* oxidase) assembly [39]).

MATERIALS AND METHODS

Materials

iO_2 sensitive probe NanO2 [40] was from Luxcel Biosciences. OptiMEM I medium, TMRM (tetramethyl rhodamine methyl ester), MTG (Mito Tracker® Green) FM, DAPI (4′,6-diamidino-2-phenylindole), Fluo-4 AM and ProLong® Gold were from Invitrogen Life Technologies. Amersham ECL™ Prime Western blotting reagent was from GE Healthcare Life Sciences; pre-made acrylamide gels, running and transfer buffer were from GenScript; BCA™ Protein Assay kit was from Thermo Fisher Scientific; protease inhibitor mixture tablets were from Roche Applied Sciences; CellTiter-Glo® ATP Assay, ImProm-II™ RT (reverse transcription) System and PCR Master Mix were from Promega. SafeView DNA stain was from NBS Biologicals. Primary antibodies were against: α-tubulin (T5168, Sigma), HIF-1α and HIF-2α (MAB1536 and AF2886, R&D Systems), HIF-1α (NB100-105, Novus Biologicals), HIF-1β (ab2771, Abcam), HIF PHD2 (4835, Cell Signalling Technology), HRP (horseradish peroxidase)-conjugated mouse anti-goat, mouse anti-rabbit and donkey anti-mouse IgG (A9452, A1949 and A0168, Sigma). Baf, CMA, DMOG (dimethyloxalylglycine), DEPC (diethyl pyrocarbonate), collagen IV, FCCP (carbonyl cyanide *p*-trifluoromethoxyphenylhydrazone) and other reagents were from Sigma–Aldrich. Primers were designed using Primer-BLAST program (http://www.ncbi.nlm.nih.gov/tools/primer-blast/) (Supplementary Table S1 at http://www.bioscirep.org/bsr/032/bsr0320587add.htm) and were synthesized by Sigma–Aldrich. Plasticware was from Sarstedt, Corning Life Sciences (Corning), Ibidi and Greiner Bio One.

Tissue culture

Human colon cancer WT (HCT116 WT) cells were obtained from the European and American Collections of Cell Cultures, HCT116 *SCO2*$^{-/-}$ [41] were kindly provided by Professor P.M. Hwang (Laboratory of Cardiovascular and Cancer Genetics, National Heart Lung and Blood Institute, National Institutes of Health, Bethesda, MD, U.S.A.). Cells were maintained in the McCoy medium supplemented with 10% FBS (fetal bovine serum), 2 mM L-glutamine, 100 units/ml penicillin/100 μg/ml streptomycin (P/S) and 10 mM Hepes, pH 7.2. For iO_2 and cellular ATP measurements, WT and *SCO2*$^{-/-}$ cells were seeded in the same medium at 1×10^5 and 8×10^4 cells per well, respectively, on 96-well plates coated with PDL (poly-D-lysine, 0.01 mg/ml) and grown for 16 h prior to the experiments. For immunofluorescence analysis cells were seeded at 1×10^5 and 8×10^4 cells per well in Ibidi 12-well μ-chambers coated with a mixture of collagen IV (0.007%) and PDL (0.003%). For protein and RNA isolation cells were seeded at 1.1×10^6 (WT) and 8×10^5 (*SCO2*$^{-/-}$) cells per well on 12-well plates (Corning) pre-coated with PDL and grown for 16 h.

Monitoring of iO_2

For the iO_2 assay, cells were loaded with NanO2 probe by incubating them in a regular medium containing 10 μg/ml probe at 37 °C for 18–24 h as described [42]. Measurements were conducted at 37 °C in serum-free McCoy's medium buffered with 20 mM Hepes (pH 7.2), typically with 48 samples of adherent cells in 200 μl of the air-saturated medium (see Supplementary Figure S1). The cells were treated with Baf and other compounds for 30 min and then the plate was transferred to a TR-F (time-resolved fluorescence) plate reader Victor 2 (PerkinElmer Life Science) placed in a hypoxia chamber (Coy Scientific) equilibrated at 6% atmospheric O_2 ($\sim$60 μM dissolved O_2). Monitoring was started using 340 nm excitation and 642 nm emission filters.

Each sample well was measured repetitively every 5–10 min for 6 h by taking two intensity readings at delay times of 30 and 70 μs, using a gate time of 100 μs [43]. The TR-F intensity signals were converted into phosphorescence lifetime (τ) values as follows: $\tau = (t_1 - t_2)/\ln(F_1/F_2)$, where F_1 and F_2 are the intensity signals at delay times t_1 and t_2. The latter were related to iO_2 (μM): $[iO_2] = 66.72 \cdot \ln(37.62/(\tau - 30.24))$. From the resulting iO_2 profiles, the rate of cell deoxygenation was calculated as O_2 consumed in 1 min by 10^6 cells (nM/min per 10^6 cells).

Measurement of the mitochondrial mass and $\Delta\Psi_m$ (membrane potential), cytosolic Ca^{2+} and cellular ATP

Cells were incubated with 50 nM MTG, 20 nM TMRM and 2.5 μM Fluo-4 AM probes in OptiMEM I (supplemented with an additional 1 mM Ca^{2+}) for 30 min in CO_2 incubator at 37 °C and then measured. During the measurements, TMRM was maintained in OptiMEM at 20 nM. AM probes were de-esterified for 15 min prior to each experiment.

Mitochondrial mass, $\Delta\Psi$m and cytosolic Ca^{2+} were measured by live cell imaging of MTG, TMRM and Fluo-4 fluorescence, respectively, using an Olympus FV1000 confocal laser scanning microscope with controlled CO_2, humidity and temperature. MTG, and Fluo-4 were excited at 488 nm with emission collected at 500–550 nm. TMRM was excited at 543 nm, emission was collected with a 555–600 nm filter. In all the experiments, fluorescence and DIC (differential interference contrast) images were collected in a sequential mode with a ×60 oil immersion objective in a number of planes using 0.5 μm steps. The resulting z-stacked images were analysed using FV1000 Viewer (Olympus), Adobe Photoshop and Illustrator software.

Total cellular ATP was quantified using CellTiter-Glo® assay following the manufacturer's protocol. Briefly, the cells were lysed with CellTiterGlo® reagent and after intensive shaking the lysates were transferred to white 96-well plates (Greiner Bio One) and measured on a Victor 2 reader under standard luminescence settings. Conditions of treatment with various effectors are described in the Results section.

Immunofluorescence

Immunofluorescence analysis was performed similarly to [44]. Briefly, HCT116 cells were seeded on Ibidi chambers, grown and treated as described above, washed with PBS, fixed with 3.7 % PFA (paraformaldehyde) in PBS, quenched with 50 mM NH_4Cl, permeabilized with 0.25 % TX100, blocked with 5 % BSA, incubated with anti-HIF-1α (Novus Biologicals) primary and fluorescent anti-mouse secondary antibodies conjugated with Alexa Fluor555 dye (Invitrogen), counterstained with DAPI, mounted with ProLong® Gold and air-dried. The intensity and localization of HIF-1α staining was analysed by confocal microscopy (Olympus): DIC, DAPI and Alexa-555 images were collected with a ×60 oil immersion objective in eight planes using a 0.5 μm step in sequential mode using standard excitation and emission wavelengths. The resulting single plane (DIC) and z-stacked fluorescent images were analysed using FV1000 Viewer software (Olympus), Adobe Photoshop and Illustrator.

Protein isolation for Western blot analysis

Whole cell lysate proteins were prepared as described in [33]. Briefly, HCT116 cells grown in the McCoy's medium on 12-well plates and treated as described above, were washed twice with PBS containing phosphatase inhibitors (Active Motif) and lysed on ice with lysis buffer, containing 150 mM NaCl, 1 mM EDTA, 1 % IGEPAL® CA-630, 50 mM Hepes (pH = 7.5) and protease inhibitors. After lysate clarification by centrifugation for 10 min at 14 000 ***g*** and 4 °C, total protein concentrations were determined using BCA™ Protein Assay kit and normalized. Proteins were denatured in ×1 Laemmli loading buffer at 95 °C and separated by SDS/PAGE in 10 % and 4–20 % gradient acrylamide gels, transferred to a 0.2 μm Immobilon™-P PVDF membrane (Sigma) using a Hoefer™ TE 22 wet mini-transfer system and probed with antibodies listed above. The signals were developed with Amersham ECL™ Prime reagent and visualized on LAS-3000 Imager (Fujifilm) using Image Reader LAS-3000 2.2 software. Quantitative image analysis was performed with ImageJ program using α-tubulin signals for normalization. Images were processed with Picasa, Photoshop and Illustrator programs.

Analysis of the HIF-1α HRE (hypoxia response element)-binding activity

Nuclear and cytosolic protein fractions were prepared from the cells using Nuclear Extract Kit (Active Motif). The DNA-binding activity of HIF-1α was analysed using TransAM™ HIF-1 kit (Active Motif) according to the manufacturer's protocol. Briefly, 5 μg of proteins were applied on the 96-well plate, pre-coated with an oligonucleotide containing a HRE (5′-TACGTGCT-3′) from the *EPO* (erythropoietin) gene, and incubated for 1 h. With serial washes after each step, primary mouse anti-HIF-1α and secondary anti-mouse HRP-conjugated antibodies were sequentially applied for 1 h. Then signals were developed and absorption was measured on a TECAN plate reader at 450 nm with a reference wavelength of 655 nm.

Gene expression analysis by RT–PCR

Total RNA was isolated using an RNA isolation kit (Promega) as per the manufacturer's protocol. RT reaction was performed using ImProm-II™ RT System (Promega) at 42 °C for 1 h using 2 μg of total denatured DNA-free RNA in 50 μl reaction mixture containing RT buffer, oligo$(dT)_{15}$ primers, dNTPs, RNase inhibitor and reverse transcriptase. After heat inactivation of the enzyme, standard PCR was performed on Mastercycler (Eppendorf). PCR was carried out at low number of cycles (25–30) in order to catch a difference in the number of cDNA copies between the samples. Each reaction was performed in triplicate in three independent experiments. PCR products were separated on agarose gels, stained with SafeView probe (NBS Biologicals), visualized using gel documentation system (Hoefer) and analysed using ImageJ program.

Statistics

The data were evaluated for statistical difference using two-tailed Student's t test. A 0.01 level of confidence was accepted as

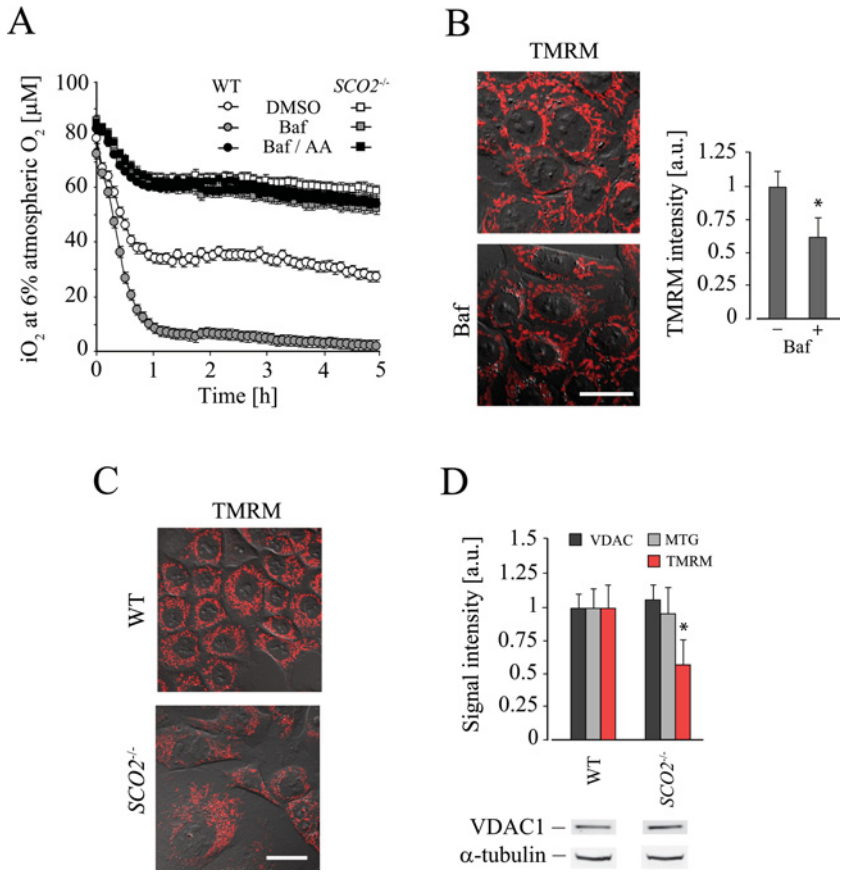

Figure 1 **Baf increases respiration in HCT116 cells through mitochondrial uncoupling**
(A) The O_2 profiles in WT and *SCO2*$^{-/-}$ HCT116 cells treated with 0.25 μM Baf at 6% hypoxia. Cells were loaded with an O_2 sensing probe NanO2 and iO_2 levels were monitored for 5 h. In control samples respiration was blocked with AA (10 μM). (B) Treatment with Baf partially depolarizes the mitochondrial membrane potential ($\Delta\Psi$m) in WT cells, as monitored by TMRM staining (20 nM in solution). (C) In *SCO2*$^{-/-}$ cells the $\Delta\Psi$m is reduced, as compared with WT. (D) A reduction in the $\Delta\Psi$m in *SCO2*$^{-/-}$ cells is not associated with a decrease in the mitochondrial size, as follows from the comparative analysis of MTG staining and VDAC1 protein levels. Bar represents 20 μm. Asterisks indicate statistical significance.

statistically significant. Plate reader data are presented as means $\pm$ S.D. for 6–8 repeated wells (error bars shown on the plots). Imaging data are presented as averages of 5–10 individual cells. All the experiments were repeated 3–5 times to ensure consistency of results.

RESULTS

Baf induces deep and sustained deoxygenation of WT HCT116 cells at 6% O_2

We reported recently that treatment with Baf induces sustained mitochondrial uncoupling and reduces iO_2 in neuronal cells [33]. Here, to find a link between mitochondrial uncoupling and O_2-dependent signalling, we first analysed the effects of atmospheric O_2 and Baf concentrations on the local deoxygenation of WT and *SCO2*$^{-/-}$ HCT116 cells. Using an iO_2 sensing probe NanO2 and TR-F plate reader Victor 2 placed in the hypoxic chamber [43], we found that at 5–8% atmospheric O_2 Baf (0.15–0.35 μM) induces profound deoxygenation of WT cells (Supplementary Figure S1 at http://www.bioscirep.org/bsr/032/bsr0320587add.htm). Thus, treatment with 0.25 μM Baf caused rapid reduction in iO_2, which remained at 0–10 μM levels for several hours (Figure 1A). Oxygenation of the cells treated with DMSO (mock) or another V-ATPase inhibitor CMA; results not shown) was significantly higher (30–40 μM). The effect of Baf was abolished by inhibition of the mitochondrial Complex III with AA (antimycin A), which brought iO_2 concentration close to the atmospheric levels ($\sim$60 μM). This respiratory response to Baf was coupled to a partial depolarization of the mitochondria ($\Delta\Psi$m), seen as a decrease in TMRM fluorescence (Figure1B). Similar to PC12 cells [33], treatment with Baf decreased pH and increased Ca^{2+} in the cytoplasm of WT HCT116 (Supplementary Figure S2 at http://www.bioscirep.org/bsr/032/bsr0320587add.htm). In contrast, for *SCO2*$^{-/-}$ cells iO_2 profiles were similar to those in WT cells treated with AA, regardless of the presence of Baf

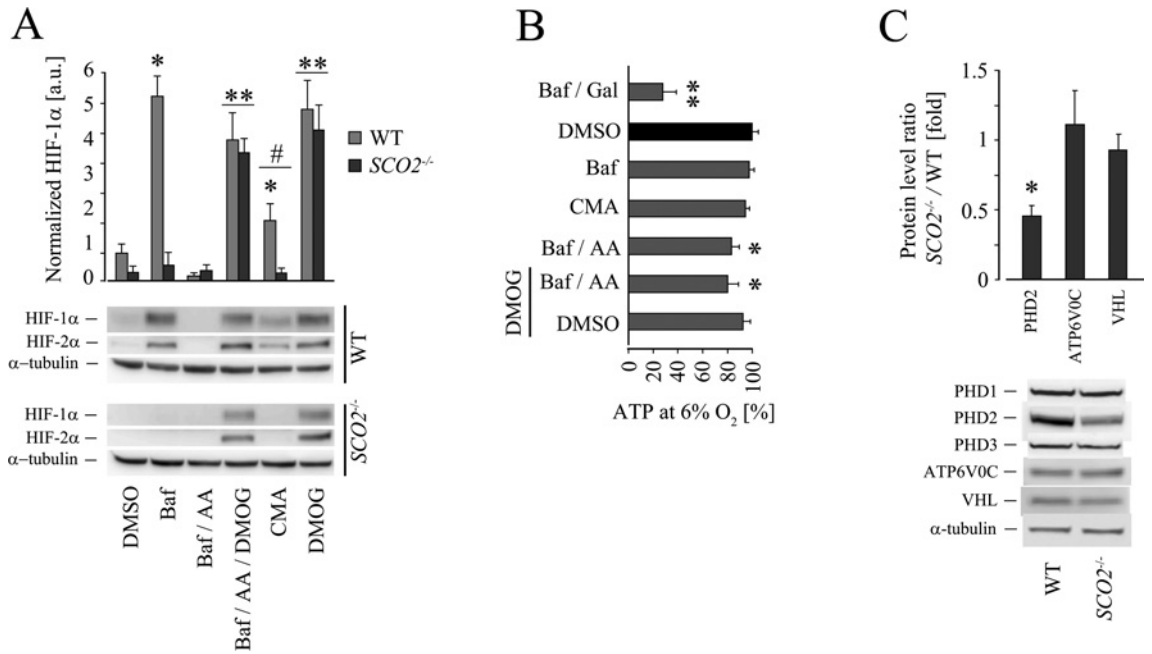

Figure 2 Stabilization of HIF-1α and HIF-2α in HCT116 cells upon Baf treatment (0.25 μM) is associated with mitochondrial uncoupling

(A) Western blot analysis demonstrates significant elevation in HIF-1α and HIF-2α levels in HCT116 WT cells treated with Baf for 5 h at 6% O_2. This effect is abolished by inhibiting mitochondrial respiration with AA. In the presence of DMOG, the level of HIF-1α and HIF-2α stabilization is similar in all samples, including those which are treated with Baf/AA. In the presence of CMA, HIF-1α and HIF-2α levels in WT cells are also increased significantly, yet to a lesser degree than upon Baf treatment. (B) Cellular ATP levels are reduced in WT cells treated with Baf/AA for 5 h at 6% O_2, regardless the presence of DMOG. Treatment with Baf in galactose (+) medium causes dramatic decrease in the ATP level. (C) The levels of PHD1, PHD3, VHL and ATP6V0C proteins are similar in WT and *SCO2*$^{-/-}$ cells, while the content of PHD2 in *SCO2*$^{-/-}$ cells is significantly lower than in WT control. Asterisks indicate statistically significant difference (*$P < 0.01$ and **$P < 0.001$, Student's *t* test) between the experimental samples and mock control (DMSO). Hash in (**A**) shows a significant difference between the effects of Baf and CMA.

(Figure 1A). This result was expected, since *SCO2*$^{-/-}$ cells deficient in the mitochondrial Complex IV [41] exhibit glycolytic type ATP production, low OCR (O_2 consumption rate) and high iO_2 levels [45].

Live cell imaging and Western blot analysis revealed no difference in the VDAC1 (voltage-dependent anion channel 1) levels and MTG fluorescence, demonstrating that relative mitochondrial mass in WT and *SCO2*$^{-/-}$ cells was similar. A decrease in TMRM staining indicated partial depolarization of the $\Delta\Psi m$ in *SCO2*$^{-/-}$ cells (Figures 1C and 1D). These data confirm that the decrease in O_2 consumption in COX-deficient cells was associated with mitochondrial respiratory malfunction rather than with changes in mitochondrial mass.

Baf induces HIF-1α and HIF-2α stabilization through mitochondrial uncoupling

Activation of the HIF-dependent pathway is a common response of the cell to the hypoxia. Therefore, we addressed a question whether the marked decrease in iO_2 induced by Baf leads to stabilization of HIF-1α and HIF-2α at 6% atmospheric O_2. We found that in WT cells treated with Baf for 5 h the levels of both HIF-α isoforms were strongly elevated (Figure 2A), as compared with mock control (DMSO) or low respiring *SCO2*$^{-/-}$ cells. Inhibition of mitochondrial respiration with AA abolished HIF-α stabilization by Baf. ATP levels in the cells treated with Baf/AA were partially reduced, suggesting that the cells experienced energy stress (Figure 2B) and could decrease *de novo* synthesis of proteins, including HIF-α subunits. To rule out this side effect, we incubated Baf/AA treated cells with DMOG, which is known to stabilize HIF-α in an O_2-independent manner through the competitive inhibition of HIF PHDs. We observed that in the presence of DMOG, HIF-1α and HIF-2α were strongly increased in all WT cells, regardless of AA treatment and ATP levels (Figure 2B). This result indicated that the effects of Baf and AA were attributable to the respiration and iO_2 levels. In agreement with this, stabilization of HIF-1α and HIF-2α in *SCO2*$^{-/-}$ cells was observed only in the presence of DMOG. This demonstrates that synthesis of HIF-1α and HIF-2α in *SCO2*$^{-/-}$ cells was preserved.

On the other hand, treatment with CMA also caused significant stabilization of HIF-α subunits in WT cells (Figure 2A). This increase was less pronounced than in the samples treated with Baf or DMOG, although it proved that HIF-α can also be stabilized by V-ATPase inhibitors as described [17]. Surprisingly, Baf and CMA had practically no effect on HIF-α

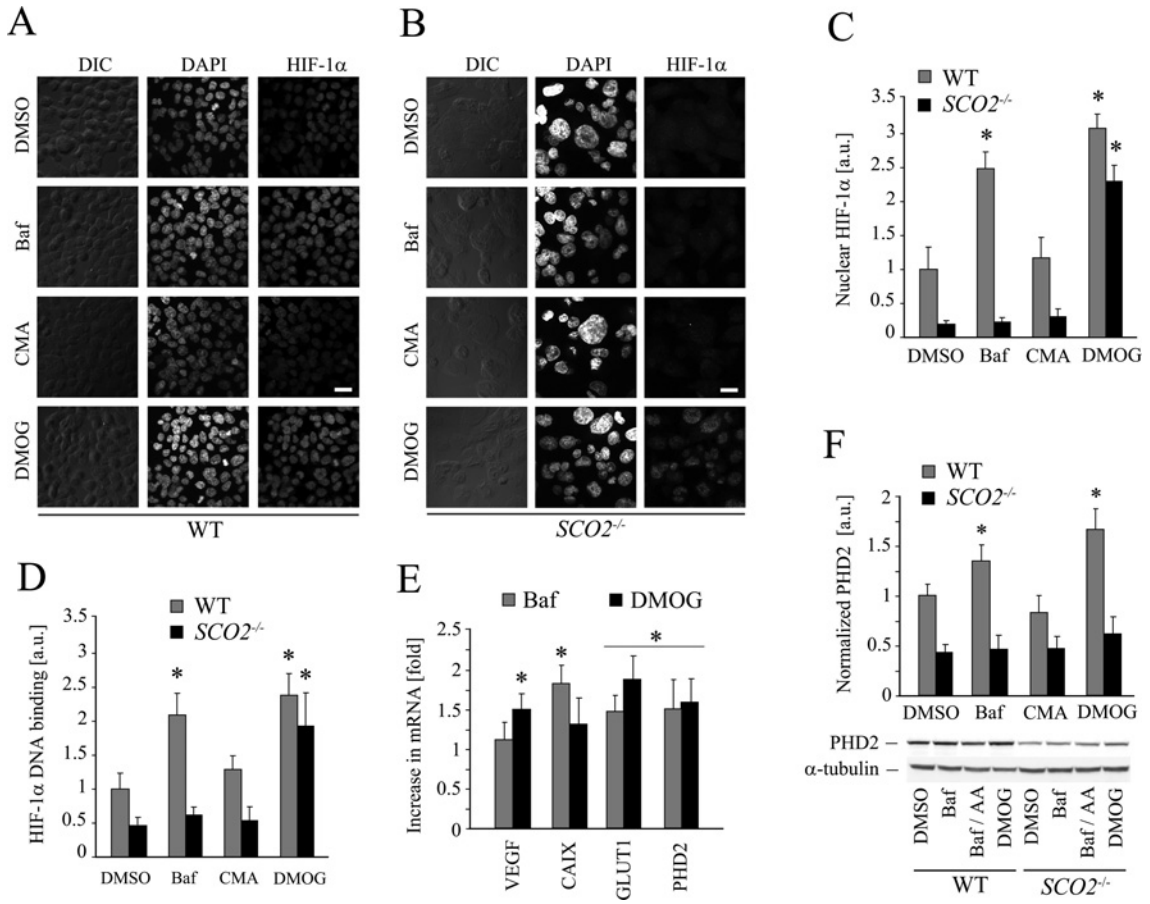

Figure 3 **Nuclear localization and functional activity of HIF-1α in the HCT116 cells treated with Baf at 6% O_2**

(A, B) Immunofluorescence analysis shows significant increase in nuclear HIF-1α staining in WT cells treated with Baf for 5 h. No effect of Baf or CMA on the nuclear HIF-1α accumulation is observed in *SCO2*$^{-/-}$ cells. Treatment with DMOG causes translocation of HIF-1 into the nuclei of both WT and *SCO2*$^{-/-}$ in an O_2-independent manner. Nuclei are counterstained with DAPI. (C) Quantitative analysis of the data shown in (A, B) is performed by measuring HIF-1-specific fluorescence in the DAPI-positive regions. (D) DNA-binding analysis using TransAM® HIF-1 kit demonstrates an increase in HIF-1-HRE interaction in WT cells upon Baf treatment. (E) Treatment with Baf activates 'hypoxia-specific' gene expression in WT cells, as demonstrated using RT–PCR analysis. Data are presented as the ratio between mRNA levels in treated and non-treated cells. (F) Western blot analysis shows that PHD2 protein level is increased in WT cells treated with Baf and DMOG; however no increase in PHD2 levels in *SCO2*$^{-/-}$ cells is observed. Asterisks indicate statistically significant difference between the experimental samples and mock control (DMSO).

stabilization in *SCO2*$^{-/-}$ cells. According to [17], Baf promotes competition of ATP6V0C with VHL protein for HIF-1α binding, thus protecting HIF-1α from PHD-dependent degradation. We hypothesized that stabilization of HIFs in the *SCO2*$^{-/-}$ cells did not occur due to a deficiency in ATP6V0C or an increase in VHL or PHD expression. However, Western blot analysis showed no difference between the two cell lines in the levels of PHD1, PHD3, ATP6V0C and VHL (Figure 2C), while PHD2 expression in *SCO2*$^{-/-}$ cells was even decreased. Under normoxia (20.9% atmospheric O_2), stabilization of HIF-1α and HIF-2α by Baf or CMA was significantly lower than under anoxia or in the presence of $CoCl_2$ (Supplementary Figure S3 at http://www.biosciresp.org/bsr/032/bsr0320587add.htm), in contrast with the effects observed under 6% O_2. Interestingly, in the cells double-treated with Baf and AA the levels of HIF-1α and HIF-2α were decreased, which was similar to the effect observed under hypoxia. This phenomenon was not associated with any ATP reduction and could be linked to the rate of mitochondrial respiration.

Baf activates HIF-dependent pathways

HIF proteins trigger adaptation of the cell to hypoxia upon translocation to the nucleus where they interact with HRE and modulate transcription of the target genes. Using immunofluorescence analysis, we evaluated the levels of nuclear HIF-1α in WT and *SCO2*$^{-/-}$ cells, treated with Baf, CMA, DMOG and DMSO for 5 h in normoxic and hypoxic conditions. At 6% atmospheric O_2 we found strong HIF-specific nuclear staining in WT cells treated with Baf and DMOG, while in *SCO2*$^{-/-}$ cells nuclear HIF-1α accumulation was observed only upon DMOG treatment (Figures 3A–3C). No detectable nuclear staining was observed

in normoxic samples unless they were incubated with DMOG (results not shown). To examine functional activity of HIF-1, we extracted nuclear proteins from the cells treated as above and performed DNA-binding ELISA analysis using TransAM® HIF-1 kit. We found that the efficiency of HIF-HRE-binding correlated with intensity of nuclear HIF-1α staining (Figures 3C and 3D). This indicates that Baf stabilizes functionally active HIF-1, which should alter the expression of target genes. To check this, we examined the effect of Baf on expression of HIF-dependent genes in hypoxic and normoxic conditions.

At 6% O_2 in WT cells treated with Baf we observed a significant increase in mRNA levels for GLUT1 (glucose transporter 1), CAIX (carbonic anhydrase IX) and PHD2, which were comparable with or higher than those in the DMOG control (Figure 3E). The level of PHD2 protein was also elevated (Figure 3F). Treatment with CMA did not affect transcription of HIF-1 target genes (results not shown). In contrast with DMOG control, treatment with Baf under normoxia moderately increased only GLUT1 mRNA level (Supplementary Table S2 at http://www.bioscirep.org/bsr/032/bsr0320587add.htm). Expression of HIF-target genes in the resting *SCO2*$^{-/-}$ cells under normoxia was practically the same as in WT cells. No changes in expression of these genes was observed in *SCO2*$^{-/-}$ cells upon treatment with Baf, while in the presence of DMOG the levels of mRNA for GLUT1, CAIX and PHD2 was moderately increased; gene expression pattern did not change at 6% O_2.

DISCUSSION

In the present study, we describe an activatory effect of moderate mitochondrial uncoupling on HIF signalling. At moderate hypoxia (6% atmospheric O_2) treatment with the K^+ ionophore Baf activates mitochondrial respiration in colon cancer HCT116 cells and strongly decreases iO_2 (Figure 1A), which is sufficient for considerable stabilization of HIF-1α and HIF-2α (Figure 2A). These results are in agreement with the previously shown key role of mitochondrial respiration in stabilization of HIF-α subunits [34–37].

Experiments with Baf and mitochondrial inhibitor AA on two cell lines exhibiting very different OCR, demonstrate that HIF-α stabilization is driven by a Baf-dependent increase in mitochondrial respiration and cell deoxygenation rather than by other cellular effects of Baf (Figure 2A). The somewhat surprising inhibitory effect of AA on HIF-α stabilization under normoxia (Supplementary Figure S3) is most probably linked to the mitochondrial activity, and needs further investigation. HIF-α stabilization is not associated exclusively with mitochondrial uncoupling; treatment with CMA partially stabilizes HIF-1α and HIF-2α in WT cells, indicating that the ATP6V0C/VHL-dependent pathway [17] also contributes to HIF-α stabilization in colon cancer cells. To our surprise, this pathway seemingly is not active in *SCO2*$^{-/-}$ cells (Figure 2A), which exhibit unchanged capacity for HIF-1α and HIF-2α production (Figure 2A, effect of DMOG). Noteworthy,

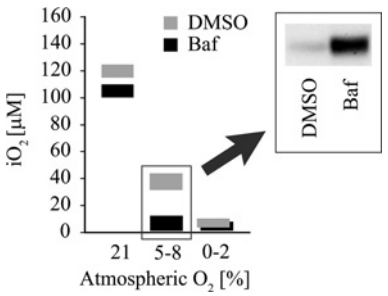

Figure 4 Proposed model for Baf-specific stabilization of HIF-α subunits in an O_2-dependent manner

At 20.9% atmospheric O_2 the levels of O_2 in the cells treated with Baf and mock (DMSO) are sufficient for hydroxylation of HIF-1α and HIF-2α, followed by PHDs-dependent degradation and/or FIH-dependent inhibition of HIFs. At 5–8% atmospheric O_2 the difference in cell oxygenation increases; upon treatment with Baf the cells become practically anoxic, which leads to stabilization of HIF-α subunits (indicated by arrow in inset) and activation of HIF pathways. At low atmospheric O_2 (0–2%) the levels of iO_2 are close to zero and HIF signalling is activated regardless of the presence of Baf.

VHL and ATP6V0C levels in *SCO2*$^{-/-}$ and WT cells do not differ (Figure 2C). Moreover, PHD2 levels in *SCO2*$^{-/-}$ cells are decreased, while PHD1 and PHD3 remain unchanged, suggesting a potentially lower rate of HIF-α hydroxylation and degradation.

In WT HCT116 cells treated with Baf under moderate hypoxia the levels of mRNA for GLUT1, PHD2 and CAIX are significantly increased (Figure 3E), indicating activation of the glycolytic proliferative pathway, which disagrees with previous work [15] in which no significant increase in mRNAs for HIF-1 target genes upon Baf treatment was seen, though their transcription was up-regulated by hypoxia. However, this mismatch has a simple explanation (Figure 4). We performed our experiments at moderate hypoxia (6% O_2), and the Baf-dependent decrease in iO_2 (by 30–40 μM, as compared with mock control, Figure 1A) was sufficient for triggering specific gene expression. In the experimental conditions described in [15], HIF signalling could be inhibited at high atmospheric O_2 by FIH asparaginyl hydroxylase, while under deep hypoxia (1% O_2) HIF-specific gene expression was already up-regulated and treatment with Baf could not increase it any further. In agreement with that, in spite of HIF-α stabilization in the presence of Baf under normoxia, we observed no significant elevation of HIF-target genes, except for a moderate increase in GLUT1 expression (Supplementary Table S2). The latter, however, most probably was HIF-independent and resulted from general activation of glycolysis upon mitochondrial uncoupling by Baf.

Recently it was shown that Baf treatment of PC12 cells is coupled with a dramatic elevation of free cytosolic Ca^{2+} due to Ca^{2+} release from acidic compartments and partially from the mitochondria [33]. In hypoxia conditions, cytosolic Ca^{2+} overload not only increases the risk of energy crisis, but can also regulate HIF signalling on transcription, translation and degradation levels (for review see [46]). In the present study, we observed substantial increases in cytosolic Ca^{2+} in HCT116 cells treated with Baf (Supplementary Figure S2). However, we did not evaluate the putative mediatory role of Ca^{2+} in Baf-dependent

stabilization of HIF-1α and HIF-2α, because inhibition of cellular Ca^{2+} fluxes decreases respiratory response to Baf and affects iO_2 levels [33].

Mitochondrial uncoupling is implicated in the cell-specific toxicity of many drugs [47]. This emphasizes the potential importance of the novel Baf-specific HIF-targeting mechanism for cancer therapy. Moreover, our results indicate that mitochondrial UCPs (uncoupling proteins), which are often expressed in tumours [48–50], may also be involved in HIF-specific regulation of cancer cell metabolism. Similar to pharmacological uncouplers, UCPs accelerate electron flow along the ETC (electron transport chain), thus elevating respiration. Uncoupling increases local O_2 gradients and iO_2, and under hypoxia may cause deep deoxygenation of the cells [38] and a decrease in tumour growth [51]. One can expect consequent stabilization of HIF-α subunits and activation of HIF signalling upon UCP up-regulation; however, to our knowledge no experimental data link together UCPs and HIF pathways [52]. Establishment of such a link is very attractive, since both UCPs and HIFs are largely involved in cancer development, including colon cancer [23,53].

AUTHOR CONTRIBUTION

Alexander Zhdanov designed and conducted experiments, performed data analysis and wrote the paper. Ruslan Dmitriev performed experiments and participated in experiment design and wrote the paper. Dmitri Papkovsky participated in experiment design and wrote the paper.

ACKNOWLEDGEMENTS

We thank Professor P. M. Hwang (National Institutes of Health) for providing us with HCT116 *SCO2*$^{-/-}$ cells, Dr Anna Golubeva (Anatomy Department, University College Cork, Cork, Ireland) for useful discussion of the results, and Ms Alicia Waters for reading the paper and making linguistic corrections prior to submission.

FUNDING

This work was supported by Science Foundation of Ireland (SFI) [grant number 07/IN.1/B1804].

REFERENCES

1 Werner, G., Hagenmaier, H., Drautz, H., Baumgartner, A. and Zahner, H. (1984) Metabolic products of microorganisms. 224. Bafilomycins, a new group of macrolide antibiotics. Production, isolation, chemical structure and biological activity. J. Antibiot. (Tokyo). **37**, 110–117
2 Bowman, E. J., Siebers, A. and Altendorf, K. (1988) Bafilomycins: a class of inhibitors of membrane ATPases from microorganisms, animal cells, and plant cells. Proc. Natl. Acad. Sci. U.S.A. **85**, 7972–7976
3 Bowman, B. J. and Bowman, E. J. (2002) Mutations in subunit C of the vacuolar ATPase confer resistance to bafilomycin and identify a conserved antibiotic binding site. J. Biol. Chem. **277**, 3965–3972
4 Bowman, E. J., Graham, L. A., Stevens, T. H. and Bowman, B. J. (2004) The bafilomycin/concanamycin binding site in subunit c of the V-ATPases from *Neurospora crassa* and *Saccharomyces cerevisiae*. J. Biol. Chem. **279**, 33131–33138
5 Kane, P. M. (2006) The where, when, and how of organelle acidification by the yeast vacuolar H^+-ATPase. Microbiol. Mol. Biol. Rev. **70**, 177–191
6 Nishi, T. and Forgac, M. (2002) The vacuolar (H^+)-ATPases–nature's most versatile proton pumps. Nat. Rev. **3**, 94–103
7 Gonzalez, A., Pfeiffer, F., Schmid, A. and Schulz, I. (1998) Effect of intracellular pH on acetylcholine-induced Ca2+ waves in mouse pancreatic acinar cells. Am. J. Physiol. **275**, C810–C817
8 Gerasimenko, J. V., Lur, G., Sherwood, M. W., Ebisui, E., Tepikin, A. V., Mikoshiba, K., Gerasimenko, O. V. and Petersen, O. H. (2009) Pancreatic protease activation by alcohol metabolite depends on Ca^{2+} release via acid store IP3 receptors. Proc. Natl. Acad. Sci. U.S.A. **106**, 10758–10763
9 Lopez, J. J., Camello-Almaraz, C., Pariente, J. A., Salido, G. M. and Rosado, J. A. (2005) Ca^{2+} accumulation into acidic organelles mediated by Ca^{2+}- and vacuolar H^+-ATPases in human platelets. Biochem. J. **390**, 243–252
10 Petersen, O. H. and Tepikin, A. V. (2008) Polarized calcium signaling in exocrine gland cells. Annu. Rev. Physiol. **70**, 273–299
11 Crompton, M. (2000) Mitochondrial intermembrane junctional complexes and their role in cell death. J. Physiol. **529**, 11–21
12 Boya, P., Gonzalez-Polo, R. A., Casares, N., Perfettini, J. L., Dessen, P., Larochette, N., Metivier, D., Meley, D., Souquere, S., Yoshimori, T. et al. (2005) Inhibition of macroautophagy triggers apoptosis. Mol. Cell. Biol. **25**, 1025–1040
13 Wu, Y. C., Wu, W. K., Li, Y., Yu, L., Li, Z. J., Wong, C. C., Li, H. T., Sung, J. J. and Cho, C. H. (2009) Inhibition of macroautophagy by bafilomycin A1 lowers proliferation and induces apoptosis in colon cancer cells. Biochem. Biophys. Res. Commun. **382**, 451–456
14 Hong, J., Nakano, Y., Yokomakura, A., Ishihara, K., Kim, S., Kang, Y. S. and Ohuchi, K. (2006) Nitric oxide production by the vacuolar-type (H+)-ATPase inhibitors bafilomycin A1 and concanamycin A and its possible role in apoptosis in RAW 264.7 cells. J. Pharmacol. Exp. Ther. **319**, 672–681
15 Lim, J. H., Park, J. W., Kim, M. S., Park, S. K., Johnson, R. S. and Chun, Y. S. (2006) Bafilomycin induces the p21-mediated growth inhibition of cancer cells under hypoxic conditions by expressing hypoxia-inducible factor-1α. Mol. Pharmacol. **70**, 1856–1865
16 Semenza, G. L. (2006) Baffled by bafilomycin: an anticancer agent that induces hypoxia-inducible factor-1α expression. Mol. Pharmacol. **70**, 1841–1843
17 Lim, J. H., Park, J. W., Kim, S. J., Kim, M. S., Park, S. K., Johnson, R. S. and Chun, Y. S. (2007) ATP6V0C competes with von Hippel–Lindau protein in hypoxia-inducible factor 1α (HIF-1α) binding and mediates HIF-1α expression by bafilomycin A1. Mol. Pharmacol. **71**, 942–948
18 Kaelin, Jr, W. G. and Ratcliffe, P. J. (2008) Oxygen sensing by metazoans: the central role of the HIF hydroxylase pathway. Mol. Cell **30**, 393–402
19 Harten, S. K., Ashcroft, M. and Maxwell, P. H. (2010) Prolyl hydroxylase domain inhibitors: a route to HIF activation and neuroprotection. Antioxid. Redox Signaling **12**, 459–480
20 Semenza, G. L. (2010) HIF-1: upstream and downstream of cancer metabolism. Curr. Opin. Genet. Dev. **20**, 51–56
21 Ban, H. S., Uto, Y. and Nakamura, H. (2010) Hypoxia-inducible factor inhibitors: a survey of recent patented compounds (2004–2010). Expert Opin. Ther. Pat. **21**, 131–146
22 Imamura, T., Kikuchi, H., Herraiz, M. T., Park, D. Y., Mizukami, Y., Mino-Kenduson, M., Lynch, M. P., Rueda, B. R., Benita, Y., Xavier, R. J. et al. (2009) HIF-1α and HIF-2α have divergent roles in colon cancer. Int. J. Cancer **124**, 763–771

23 Pez, F., Dayan, F., Durivault, J., Kaniewski, B., Aimond, G., Le Provost, G. S., Deux, B., Clezardin, P., Sommer, P., Pouyssegur, J. et al. (2011) The HIF-1-inducible lysyl oxidase activates HIF-1 via the Akt pathway in a positive regulation loop and synergizes with HIF-1 in promoting tumor cell growth. Cancer Res. **71**, 1647–1657
24 Burkitt, K., Chun, S. Y., Dang, D. T. and Dang, L. H. (2009) Targeting both HIF-1 and HIF-2 in human colon cancer cells improves tumor response to sunitinib treatment. Mol. Cancer Ther. **8**, 1148–1156
25 Brown, J. M. and Wilson, W. R. (2004) Exploiting tumour hypoxia in cancer treatment. Nat. Rev. Cancer **4**, 437–447
26 Bertout, J. A., Patel, S. A. and Simon, M. C. (2008) The impact of O2 availability on human cancer. Nat. Rev. Cancer **8**, 967–975
27 Holmquist-Mengelbier, L., Fredlund, E., Lofstedt, T., Noguera, R., Navarro, S., Nilsson, H., Pietras, A., Vallon-Christersson, J., Borg, A., Gradin, K. et al. (2006) Recruitment of HIF-1α and HIF-2α to common target genes is differentially regulated in neuroblastoma: HIF-2α promotes an aggressive phenotype. Cancer Cell **10**, 413–423
28 Giatromanolaki, A., Koukourakis, M. I., Sivridis, E., Turley, H., Talks, K., Pezzella, F., Gatter, K. C. and Harris, A. L. (2001) Relation of hypoxia inducible factor 1 α and 2 α in operable non-small cell lung cancer to angiogenic/molecular profile of tumours and survival. Br. J. Cancer **85**, 881–890
29 Keith, B., Johnson, R. S. and Simon, M. C. (2010) HIF1α and HIF2α: sibling rivalry in hypoxic tumour growth and progression. Nat. Rev. Cancer **12**, 9–22
30 Beasley, N. J., Leek, R., Alam, M., Turley, H., Cox, G. J., Gatter, K., Millard, P., Fuggle, S. and Harris, A. L. (2002) Hypoxia-inducible factors HIF-1α and HIF-2α in head and neck cancer: relationship to tumor biology and treatment outcome in surgically resected patients. Cancer Res. **62**, 2493–2497
31 Volm, M. and Koomagi, R. (2000) Hypoxia-inducible factor (HIF-1) and its relationship to apoptosis and proliferation in lung cancer. Anticancer Res. **20**, 1527–1533
32 Teplova, V. V., Tonshin, A. A., Grigoriev, P. A., Saris, N. E. and Salkinoja-Salonen, M. S. (2007) Bafilomycin A1 is a potassium ionophore that impairs mitochondrial functions. J. Bioenerg. Biomembr. **39**, 321–329
33 Zhdanov, A. V., Dmitriev, R. I. and Papkovsky, D. B. (2011) Bafilomycin A1 activates respiration of neuronal cells via uncoupling associated with flickering depolarization of mitochondria. Cell. Mol. Life Sci. **68**, 903–917
34 Brown, S. T. and Nurse, C. A. (2008) Induction of HIF-2α is dependent on mitochondrial O_2 consumption in an O_2-sensitive adrenomedullary chromaffin cell line. Am. J. Physiol. Cell Physiol. **294**, C1305–C1312
35 Hagen, T., Taylor, C. T., Lam, F. and Moncada, S. (2003) Redistribution of intracellular oxygen in hypoxia by nitric oxide: effect on HIF1α. Science **302**, 1975–1978
36 Doege, K., Heine, S., Jensen, I., Jelkmann, W. and Metzen, E. (2005) Inhibition of mitochondrial respiration elevates oxygen concentration but leaves regulation of hypoxia-inducible factor (HIF) intact. Blood **106**, 2311–2317
37 Chua, Y. L., Dufour, E., Dassa, E. P., Rustin, P., Jacobs, H. T., Taylor, C. T. and Hagen, T. (2010) Stabilization of hypoxia-inducible factor-1α protein in hypoxia occurs independently of mitochondrial reactive oxygen species production. J. Biol. Chem. **285**, 31277–31284
38 Zhdanov, A. V., Ogurtsov, V. I., Taylor, C. T. and Papkovsky, D. B. (2010) Monitoring of cell oxygenation and responses to metabolic stimulation by intracellular oxygen sensing technique. Integr. Biol.. **2**, 443–451
39 Matoba, S., Kang, J. G., Patino, W. D., Wragg, A., Boehm, M., Gavrilova, O., Hurley, P. J., Bunz, F. and Hwang, P. M. (2006) p53 regulates mitochondrial respiration. Science **312**, 1650–1653
40 Fercher, A., Borisov, S. M., Zhdanov, A. V., Klimant, I. and Papkovsky, D. B. (2011) Intracellular O_2 sensing probe based on cell-penetrating phosphorescent nanoparticles. ACS Nano **5**, 5499–5508
41 Matsumoto, T., Wang, P. Y., Ma, W., Sung, H. J., Matoba, S. and Hwang, P. M. (2009) Polo-like kinases mediate cell survival in mitochondrial dysfunction. Proc. Natl. Acad. Sci. U.S.A. **106**, 14542–14546
42 Zhdanov, A. V., Ward, M. W., Prehn, J. H. and Papkovsky, D. B. (2008) Dynamics of intracellular oxygen in PC12 Cells upon stimulation of neurotransmission. J. Biol. Chem. **283**, 5650–5661
43 O'Riordan, T. C., Zhdanov, A. V., Ponomarev, G. V. and Papkovsky, D. B. (2007) Analysis of intracellular oxygen and metabolic responses of Mammalian cells by time-resolved fluorometry. Anal. Chem. **79**, 9414–9419
44 Dmitriev, R. I., Okkelman, I. A., Abdulin, R. A., Shakhparonov, M. I. and Pestov, N. B. (2009) Nuclear transport of protein TTC4 depends on the cell cycle. Cell Tissue Res. **336**, 521–527
45 Sung, H. J., Ma, W., Wang, P. Y., Hynes, J., O'Riordan, T. C., Combs, C. A., McCoy, J. P. Jr., Bunz, F., Kang, J. G. and Hwang, P. M. (2010) Mitochondrial respiration protects against oxygen-associated DNA damage. Nat. Commun. **1**, 5
46 Yee Koh, M., Spivak-Kroizman, T. R. and Powis, G. (2008) HIF-1 regulation: not so easy come, easy go. Trends Biochem. Sci. **33**, 526–534
47 Dykens, J. A. and Will, Y. (2007) The significance of mitochondrial toxicity testing in drug development. Drug Discovery Today **12**, 777–785
48 Horimoto, M., Resnick, M. B., Konkin, T. A., Routhier, J., Wands, J. R. and Baffy, G. (2004) Expression of uncoupling protein-2 in human colon cancer. Clin. Cancer Res. **10**, 6203–6207
49 Harper, M. E., Antoniou, A., Villalobos-Menuey, E., Russo, A., Trauger, R., Vendemelio, M., George, A., Bartholomew, R., Carlo, D., Shaikh, A. et al. (2002) Characterization of a novel metabolic strategy used by drug-resistant tumor cells. FASEB J. **16**, 1550–1557
50 Samudio, I., Fiegl, M. and Andreeff, M. (2009) Mitochondrial uncoupling and the Warburg effect: molecular basis for the reprogramming of cancer cell metabolism. Cancer Res. **69**, 2163–2166
51 Chen, Y., Cairns, R., Papandreou, I., Koong, A. and Denko, N. C. (2009) Oxygen consumption can regulate the growth of tumors, a new perspective on the Warburg effect. PLoS ONE **4**, e7033
52 Baffy, G. (2010) Uncoupling protein-2 and cancer. Mitochondrion **10**, 243–252
53 Kuai, X. Y., Ji, Z. Y. and Zhang, H. J. (2010) Mitochondrial uncoupling protein 2 expression in colon cancer and its clinical significance. World J. Gastroenterol. **16**, 5773–5778

Received 31 July 2012; accepted 1 August 2012
Published as Immediate Publication 3 September 2012, doi 10.1042/BSR20120085

Biosci. Rep. (2012) / **32** / 587–595 (Printed in Great Britain) / doi 10.1042/BSR20120085

online data

Original Paper

SUPPLEMENTARY ONLINE DATA

Bafilomycin A1 activates HIF-dependent signalling in human colon cancer cells via mitochondrial uncoupling

Alexander V. ZHDANOV[1], Ruslan I. DMITRIEV and Dmitri B. PAPKOVSKY

Biochemistry Department, University College Cork, Cork, Ireland

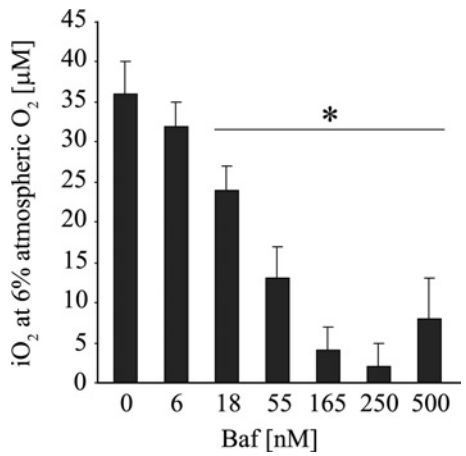

Figure S1 Baf increases cellular respiration in a concentration-dependent manner

Experiment was conducted in a hypoxia chamber at 6% atmospheric O_2. Asterisk indicates significant difference.

[1] To whom correspondence should be addressed (email a.zhdanov@ucc.ie).

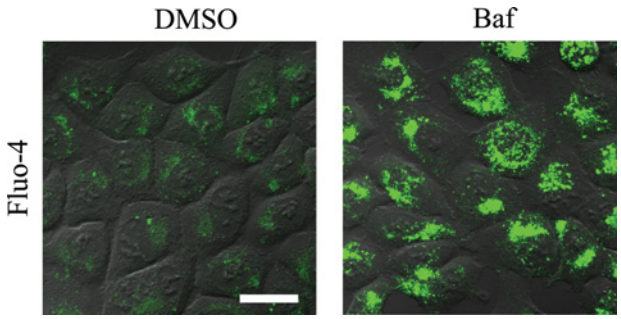

Figure S2 Treatment with Baf induces 3.5-fold increase in Fluo-4 intensity, reflecting strong elevation of cytosolic Ca^{2+}
Live cell confocal images of the cells treated with 0.25 μM Baf or mock (DMSO) for 1.5 h, z-stack of two planes. Bar represents 20 μm.

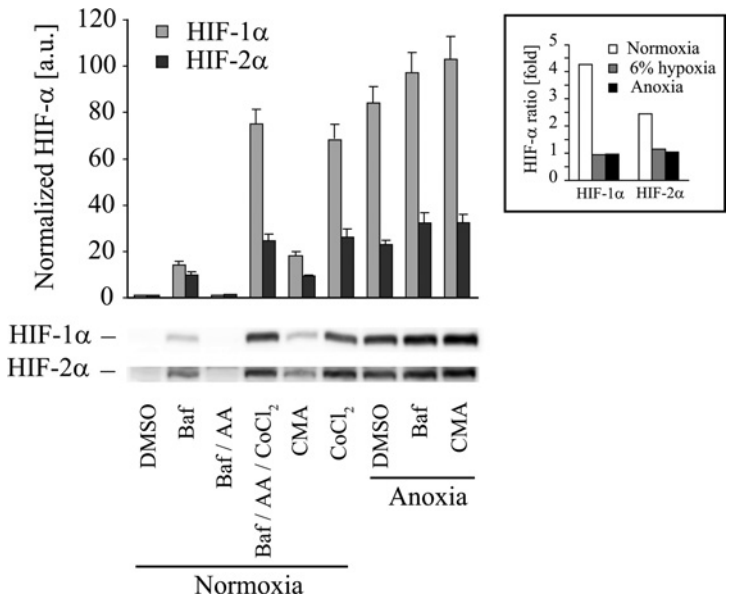

Figure S3 Baf-dependent stabilization of HIF-α in normoxia is substantially lower than in anoxia or on treatment with $CoCl_2$
Effects of Baf and CMA are similar. Inset, ratio between HIF levels upon treatment with Baf (0.25 μM) and $CoCl_2$ (200 μM) is shown.

Table S1 Primers used for analysis of gene expression by RT-PCR
ATCB, β-actin; LDHA, lactate dehydrogenase.

Genes	Forward primer	Reverse primer
VEGFA	5′-GTGTGCGCAGACAGTGCTCCAG-3′	5′-AGGAAGCTCATCTCTCCTATGTGCTG-3′
GLUT-1	5′-CAGCAGCCTGTGTATGCCACCA-3′	5′-AAGCCGGAAGCGATCTCATCGA-3′
LDHA	5′-GTGCCATCAGTATCTTAATGAAGGACTTG-3′	5′-TCCAAGCCACGTAGGTCAAGATATCC-3′
ATCB	5′-GAGCGGGAAATCGTGCGTGACA-3′	5′-GTACATGGTGGTGCCGCCAGAC-3′
CAIX	5′-GGCGAGGAGGATCTGCCCA-3′	5′-GTGGCCATTGTTGCGCAGGC-3′
PHD2	5′- CAAGCTCGTGTGCCAGGGCA-3′	5′- GCCCGTCCGTGAACTTCCCG-3′
PHD3	5′- CTGGAGCGCGTCAAGCAGCT-3′	5′- TTGGGGTTGTCCACGTGGCG-3′
PDK1	5′-TGCGGCAAGAGTTGCCTGTCAG-3′	5′-GCTGGTGACAGGATCCACCCCA-3′

Table S2 Gene expression levels in HCT116 cells, WT (at 20.9% O_2) and *SCO2*$^{-/-}$ (at 6 and 20.9% O_2)
Results are normalized to mock control (WT cells treated with DMSO). LDHA, lactate dehydrogenase.

Cell type	Atmospheric O_2 level	Treatment	Genes			
			GLUT1	LDHA	CAIX	PHD2
SCO2$^{-/-}$	20.9%	DMSO	1 ± 0.1	0.9 ± 0.2	0.6 ± 0.3	1.1 ± 0.3
		Baf	1.1 ± 0.2	1.1 ± 0.2	0.8 ± 0.2	1.1 ± 0.2
		DMOG	1.6 ± 0.3	1.2 ± 0.1	1.3 ± 0.6	1.4 ± 0.1
	6%	DMSO	1.1 ± 0.2	1 ± 0.2	0.9 ± 0.2	0.8 ± 0.1
		Baf	1.1 ± 0.2	1.1 ± 0.2	1.1 ± 0.1	1 ± 0.1
		DMOG	1.6 ± 0.2	1.3 ± 0.3	1.4 ± 0.2	1.6 ± 0.2
WT	20.9%	DMSO	1 ± 0.1	1 ± 0.1	1 ± 0.1	1 ± 0.1
		Baf	1.3 ± 0.2	1 ± 0.1	1.2 ± 0.2	1.1 ± 0.1
		DMOG	1.7 ± 0.2	1.5 ± 0.2	1.9 ± 0.2	2.2 ± 0.1

Received 31 July 2012; accepted 1 August 2012
Published as Immediate Publication 3 September 2012, doi 10.1042/BSR20120085